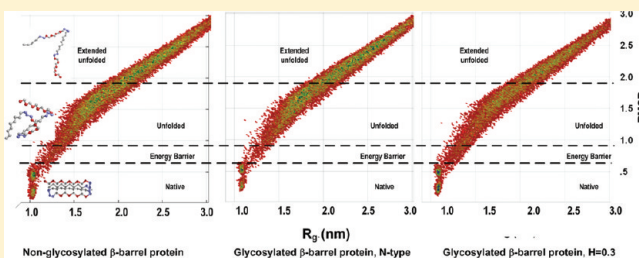


# How Hydrophobicity and the Glycosylation Site of Glycans Affect Protein Folding and Stability: A Molecular Dynamics Simulation

Diannan Lu, Cheng Yang, and Zheng Liu\*

Department of Chemical Engineering, Tsinghua University, Beijing, 100084, China

**ABSTRACT:** Glycosylation is one of the most common post-translational modifications in the biosynthesis of protein, but its effect on the protein conformational transitions underpinning folding and stabilization is poorly understood. In this study, we present a coarse-grained off-lattice 46- $\beta$  barrel model protein glycosylated by glycans with different hydrophobicity and glycosylation sites to examine the effect of glycans on protein folding and stabilization using a Langevin dynamics simulation, in which an  $H$  term was proposed as the index of the hydrophobicity of glycan. Compared with its native counterpart, introducing glycans of suitable hydrophobicity ( $0.1 < H < 0.4$ ) at flexible peptide residues of this model protein not only facilitated folding of the protein but also increased its conformation stability significantly. On the contrary, when glycans were introduced at the restricted peptide residues of the protein, only those hydrophilic ( $H = 0$ ) or very weak hydrophobic ( $H < 0.2$ ) ones contributed slightly to protein stability but hindered protein folding due to increased free energy barriers. The glycosylated protein retained the two-step folding mechanism in terms of hydrophobic collapse and structural rearrangement. Glycan chains located in a suitable site with an appropriate hydrophobicity facilitated both collapse and rearrangement, whereas others, though accelerating collapse, hindered rearrangement. In addition to entropy effects, that is, narrowing the space of the conformations of the unfolded state, the presence of glycans with suitable hydrophobicity at suitable glycosylation site strengthened the folded state via hydrophobic interaction, that is, the enthalpy effect. The simulations have shown both the stabilization and the destabilization effects of glycosylation, as experimentally reported in the literature, and provided molecular insight into glycosylated proteins. The understanding of the effects of glycans with different hydrophobicities on the folding and stability of protein, as attempted by the present work, is helpful not only to explain the stabilization and destabilization effect of real glycoproteins but also to design protein–polymer conjugates for biotechnological purposes.



## INTRODUCTION

Glycosylation is one of the most important post-translational modifications of new synthesized proteins in the cell, regulating their function by modulating their biophysical properties.<sup>1–3</sup> Numerous experiments have revealed that glycosylation can alter the thermodynamic, kinetic, and structural features of proteins, enhancing their structure and function beyond that dictated by their sequence.<sup>1,4,5</sup> Glycosylation is an effective way to generate homologous proteins for various applications.

Glycosylation occurs during or after protein synthesis and is a complex process that involves 13 different kinds of monosaccharides attached to eight types of amino acid residues.<sup>5</sup> Some important enzymes, such as glucosidase,<sup>6</sup> glucosyltransferase,<sup>7</sup> and endo-N-acetyl- $\beta$ -D-glucosaminidase,<sup>8,9</sup> are involved in the glycosylation process and catalyze the formation or breakage of different glycosidic bonds. Among their functional roles, glycans serve as recognition makers,<sup>10</sup> mediate interactions with pathogens,<sup>11,12</sup> modulate immune responses,<sup>13,14</sup> and regulate protein turnovers.<sup>15,16</sup> There are two kinds of glycan linkages: N-linked glycan and O-linked glycan.<sup>5</sup> N-Linked glycans are attached to the side-chain nitrogen of asparagine residues in the sequence Asn-X-Ser/Thr (X must not be proline) as the newly synthesized polypeptide is translated through the membrane into the lumen of the endoplasmic reticulum,<sup>17</sup> although not every sequon is glycosylated. The homogeneous

sugar is then trimmed down and subsequently modified in the Golgi apparatus, leading to the many heterogeneous forms of N-linked glycans. Less commonly, sugars are linked to the hydroxyl groups of serine, threonine, tyrosine, hydroxyproline, hydroxylysine, or another hydroxylated amino acid. These linkages are formed in the Golgi apparatus by less well-understood pathways. Glycosylphosphatidylinositol (GPI) anchors can be attached to the carboxyl terminus of glycoproteins.<sup>18</sup> In this process, a carboxy-terminal transmembrane segment of the protein is cleaved and replaced with the GPI anchor such that the protein remains in the membrane.<sup>19,20</sup>

For N-linked glycoproteins, the glycan is added to the unfolded protein while it is in the translocon complex,<sup>17</sup> suggesting that glycans might assist protein folding in vivo. However, this “chaperone-like” behavior of glycan remains ambiguous; some glycoproteins, such as human ST3Gal I,<sup>21</sup> GD3 synthase (ST8Sia I),<sup>22</sup> hepatitis C virus envelope proteins,<sup>23</sup> *Bombyx mori* nucleopolyhedrovirus V-CATH,<sup>24</sup> and tripeptidyl-peptidase I,<sup>25</sup> misfold and aggregate in the absence of glycans, whereas in other proteins elimination of some or all glycans has no effect on folding. For example, in *Antheraea pernyi* arylphorin,

Received: April 28, 2011

Revised: October 30, 2011

Published: November 27, 2011

glycosylation of Asn(344) is crucial for the folding process; however, glycosylation of Asn(196) is not.<sup>26</sup> These seemingly conflicting results indicate the importance of glycosylation sites, although these are poorly understood, particularly at the molecular level.

It is interesting to note the diverse results of experiments on the impact of composition and length of glycans on the stabilization and folding of proteins.<sup>27</sup> Glycans have been recognized as bulky hydrophilic polymers that increase the solubility of proteins and resist proteolysis. Recent results, however, have demonstrated that some glycans are hydrophobic and alter the thermal and kinetic stability of proteins and even their folding pathways.<sup>28</sup> Although glycosylation of a protein generally increases its thermodynamic stability compared with that of nonglycosylated protein,<sup>29–31</sup> glycosylation of specific sites on some proteins, such as Asn(132) in CD14, has no effect on stability.<sup>32</sup> The reduction in thermodynamic stability after glycosylation has been demonstrated for tyrosinase and tyrosinase-related proteins.<sup>33,34</sup> These conflicting experimental results have caused controversy over whether glycans affect entropy or enthalpy and whether these effects occur mainly on the folded or unfolded state.

The funneled energy landscape theory states that a new synthetic polypeptide folds by navigating through an energy landscape that is globally funneled toward a structurally defined native state. This is widely accepted to explain and predict the folding thermodynamics and kinetics of many proteins.<sup>30</sup> The energy landscape theory also explains the increased thermal stability conferred by glycosylation from the viewpoint of either the decrease of enthalpy or the increase of entropy of the folded protein. Alternatively, glycosylation increases protein stability by destabilizing the unfolded state via decreasing its entropy or increasing its enthalpy.<sup>30,31</sup> Choi et al.<sup>35</sup> and Fernandez-Tejada et al.<sup>36,37</sup> have conducted molecular simulations of glycoproteins using all-atom models to study protein stability and folding. More recently, a coarse-grained model of the SH domain with six possible glycosylation sites was established by Shental-Bechor and Levy.<sup>38</sup> In this model, two types of polysaccharides were used: one with five sugar rings and a single branch, and another with 11 sugar rings and two branches. The effects of the number of glycosylations and their location on the stability of the protein and its folding mechanism were studied. It was concluded that the glycans increased protein stability primarily by increasing the enthalpy of unfolded states.<sup>38</sup> Cheng et al. conducted an all-atom molecular dynamics simulation to study the collapse of a peptide linked to a single *N*-glycan.<sup>28</sup> It was shown that enhancement of the hydrophobic collapse compensated for the weakened entropic coiling due to the bulky glycan chain and led to stronger burial of the hydrophobic surface.<sup>28</sup> However, most published studies have investigated isolated monomeric proteins, which account for a small fraction of protein types in the cell.

The energy landscape theory offers a universal physical basis for understanding protein folding and aggregation and is used to illustrate the intra- and intermolecular events that underpin folding thermodynamics and kinetics. Here we apply the energy landscape theory to explore the effects of glycosylation on the conformational transition underlying protein stabilization and folding *in vitro* and *in vivo*. The  $\beta$ -barrel protein, which has 10 possible glycosylated variants, was used as the model protein to examine the effects of the type of glycan and site of glycosylation on stability and folding. The  $\beta$ -barrel protein comprises three different types of residue, and glycan includes 14 sugar rings and three branches. We added glycans to the different glycosylation sites of the  $\beta$ -barrel protein and studied the effects of their

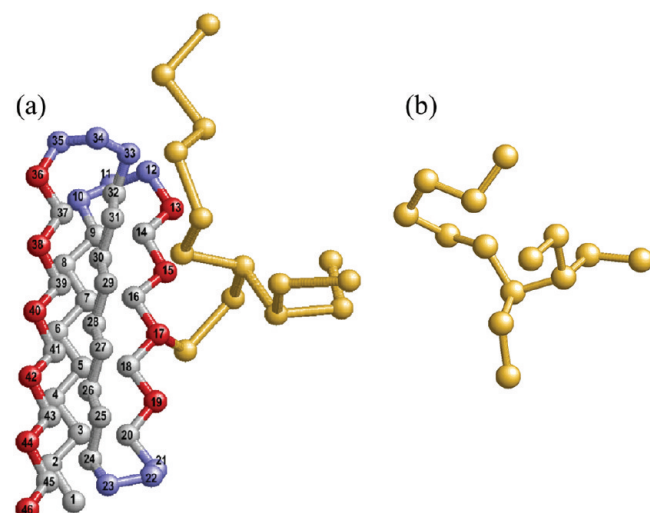


**Figure 1.** Molecular model of glycosylated  $\beta$ -barrel protein and glycan. (a) Native structure of glycosylated  $\beta$ -barrel protein. Red: hydrophilic amino acid residue; gray: hydrophobic amino acid residue; blue: neutral amino acid residue; yellow: sugar unit. The radius of each amino acid residue is 0.38 nm; (b) N-linked glycan comprising Glc<sub>3</sub>Man<sub>9</sub>GlcNAc<sub>2</sub>. The radius of each sugar unit is 0.6 nm.

location and properties on the stability and folding behavior of the protein and its folding mechanism. An *H* term was proposed to describe the hydrophobicity of glycan. It is noted here that, due to the lack of atomic details, it is hard to correlate the simulation results with specific real proteins. However, this modeling procedure grasped one essential nature of glycoproteins, that is, the interaction between protein and glycans. Thus the simulation of this model protein would benefit not only the understanding the folding behavior and stability of glycoproteins but also to design of novel glycoproteins or protein–polymer conjugate for biotechnology purposes.

## MATERIALS AND METHODS

**Glycoprotein Model.** In this study, glycosylation occurred on the hydrophilic amino acid residues of the G $\ddot{\text{o}}$ -like  $\beta$ -barrel protein, which is used extensively for the study of protein folding in bulk solution<sup>39,40</sup> and confinement,<sup>41,42</sup> molecular chaperone-assisted protein folding,<sup>43,44</sup> and protein aggregation.<sup>42,45</sup> Figure 1 shows a typical glycosylated  $\beta$ -barrel protein, in which amino acid residues and sugar units are represented by spherical beads of radius 0.38 nm and 0.60 nm, respectively. The side chains of the amino acid residues are not considered explicitly. The native structure of this model protein was obtained by a simulated annealing method. The protein portion of glycosylated protein contains 46 beads that are divided into three groups denoted as hydrophobic ( $H_p$ , colored gray), polar ( $P_p$ , colored red), and neutral ( $N_p$ , colored blue). The addition of glycans did not alter the native conformation of  $\beta$ -barrel protein when the temperature was below 300 K. The glycan portion of glycosylated protein contains 14 beads that are homogeneous with tunable hydrophobicity denoted as *H*. In this study, the value of *H* ranged from 0.0 to 0.4. When *H* is equal to 0.0, the glycan is hydrophilic and denoted as N-type glycans (N beads). Although this simplified model cannot give detailed information of glycoprotein at an all-atom level, the simulation of this model protein, which captures the physical nature of glycosylated protein, can generate molecular

insight into the general effects of the glycan on the folding and stability of glycosylated proteins.

As described elsewhere,<sup>41</sup> the Hamiltonian of the  $\beta$ -barrel protein comprises bond energy, excluded volume effects, and long-range van der Waals attractions. Specially, the bond fluctuation is described by a harmonic potential as

$$V_b = \sum_{\text{bonds}} k_b(r - \sigma)^2 \quad (1)$$

where  $r$  is the center-to-center distance between two nearest neighboring amino acid residues,  $\sigma$  is the equilibrium bond length, and  $k_b = 100\varepsilon_h$  is the bond spring constant. In this study,  $\varepsilon_h$  and  $\sigma$  are 5.0 kJ/mol and 0.38 nm, respectively.

The bending potential specifies the energy associated with the fluctuation of the bond angles. It is also expressed as in a harmonic form as

$$V_\theta = \sum_{\text{bond angles}} k_\theta(\theta - \theta_0)^2 \quad (2)$$

where  $\theta$  denotes the bond angles,  $\theta_0 = 105^\circ$  is the equilibrium bond angle, and  $k_\theta = 10\varepsilon_h/(\text{rad})^2$ . The dihedral potential is described by

$$V_\varphi = \sum_{\text{dihedral angles}} [k_\varphi^{(1)}(1 + \cos \varphi) + k_\varphi^{(2)}(1 + \cos 3\varphi)] \quad (3)$$

where  $k_\varphi^{(1)} = 0$  and  $k_\varphi^{(2)} = 0.2\varepsilon_h$  if more than one of the four beads of protein defining the dihedral angle  $\varphi$  is neutral (colored blue in Figure 1a), and  $k_\varphi^{(2)} = k_\varphi^{(2)} = 1.2\varepsilon_h$  otherwise. The dihedral potential exhibits a minimum in the trans or gauche configurations. These energy minima are responsible for the formation of  $\beta$ -turns in the native structure of the model protein.

The “non-bonded” pair interaction includes the excluded volume effect and the long-range van der Waals attraction, which takes the form of Lennard-Jones (LJ)-like potential when applied to amino-acid residues separated by at least two peptide bonds

$$V_{\text{LJ}} = \sum_{\text{LJ}} 4\varepsilon_h \left[ A_{ij} \left( \frac{\sigma}{r} \right)^{12} - B_{ij} \left( \frac{\sigma}{r} \right)^6 \right] \quad (4)$$

where the dimensionless parameters  $A_{ij}$  and  $B_{ij}$  depend on the identities of interacting beads. Here we adopted  $A_{ij} = 1/3$  and  $B_{ij} = -1$  for the P<sub>P</sub>H<sub>P</sub> and P<sub>P</sub>P<sub>P</sub> pairs;  $A_{ij} = 1$  and  $A_{ij} = 0$  for the H<sub>P</sub>N<sub>P</sub>, P<sub>P</sub>N<sub>P</sub>, and N<sub>P</sub>N<sub>P</sub> pairs, and  $A_{ij} = 1$  and  $A_{ij} = 1$  for the interaction between H<sub>P</sub>H<sub>P</sub> pairs. To avoid the frustrated conformations, we consider only nonbonded H<sub>P</sub>H<sub>P</sub> pairs with a center-to-center distance below 1.167 $\sigma$  in the native structure. Table 1 gives 47 pairs of amino-acid monomers that are defined as the native contacts, most involving hydrophobic residues buried in the protein core.

The energy term of the glycan of glycosylated protein includes bond energy, angle potential, and an excluded volume effects and long-range van der Waals attractions. Specially, the bond fluctuation of glycan is described by a harmonic potential as

$$V_{bg} = \sum_{\text{bonds}} k_{bg}(r_g - \sigma_g)^2 \quad (5)$$

where  $r_g$  is the center-to-center distance between two nearest neighboring sugar units,  $\sigma_g = 0.6$  nm is the equilibrium bond length, and  $k_{bg} = 100\varepsilon_h$  is the bond spring constant.

**Table 1. Indices of Native Contacts in the Protein Portion of the Glycosylated Protein Model**

native contacts			
(1, 24)	(1, 45)		
(2, 24)	(2, 43)	(2, 45)	
(3, 20)	(3, 24)	(3, 26)	(3, 43)
(4, 26)	(4, 41)	(4, 43)	
(5, 18)	(5, 26)	(5, 28)	(5, 41)
(6, 28)	(6, 39)	(6, 41)	
(7, 16)	(7, 28)	(7, 30)	(7, 39)
(8, 30)			
(9, 14)	(9, 30)	(9, 32)	(9, 37)
(14, 32)			
(16, 28)	(16, 29)	(16, 30)	
(18, 26)	(18, 27)	(18, 28)	
(20, 24)	(20, 25)		
(24, 45)			
(25, 43)			
(26, 41)		(26, 43)	
(27, 41)			
(28, 39)		(28, 41)	
(29, 39)			
(30, 39)			
(31, 37)			

The bending potential specifies the energy associated with the fluctuation of the bond angles. It is also expressed in a harmonic form as

$$V_{\theta g} = \sum_{\text{bond angles}} k_{\theta g}(\theta_g - \theta_{0g})^2 \quad (6)$$

where  $\theta_g$  denotes the bond angles,  $\theta_{0g} = 105^\circ$  is the equilibrium bond angle, and  $k_{\theta g} = 10\varepsilon_h/(\text{rad})^2$ .

The LJ-like potential is applied to represent nonbonded interaction between sugar units separated by at least two connected bonds

$$V_{\text{LJg}} = \sum_{\text{LJ}} 4\varepsilon_h \left[ \left( \frac{\sigma_g}{r_g} \right)^{12} - H \left( \frac{\sigma_g}{r_g} \right)^6 \right] \quad (7)$$

where  $r_g$  and  $\sigma_g = 0.6$  nm are the center-to-center distance and equilibrium distance between sugar units, respectively. The dimensionless parameter  $H$  represents the hydrophobicity of glycan. In this study, the value of  $H$  ranged from 0.0 to 0.4. When  $H$  is equal to 0.0, the glycan is hydrophilic.

The interaction between protein and glycan includes bond energy and excluded volume effects and long-range van der Waals attractions. The bond energy only occurs between amino acid and the sugar unit where glycosylation occurs. The bond fluctuation of glycan is described by a harmonic potential as

$$V_{\text{bpg}} = \sum_{\text{bonds}} k_{\text{bpg}}(r_{\text{pg}} - \sigma_{\text{pg}})^2 \quad (8)$$

where  $r_{\text{pg}}$  is the center-to-center distance between connected amino acid and sugar unit,  $\sigma_{\text{pg}} = (\sigma + \sigma_g)/2$  is the equilibrium bond length, and  $k_{\text{bpg}} = (k_b \times k_{bg})^{1/2}$  is the bond spring constant.

The LJ-like potential is applied to represent nonbonded interactions between sugar units and amino acid

$$V_{\text{LJ}_{\text{pg}}} = \sum_{\text{LJ}} 4\varepsilon_h \left[ \left( \frac{\sigma_{\text{pg}}}{r_{\text{pg}}} \right)^{12} - H_{\text{pg}} \left( \frac{\sigma_{\text{pg}}}{r_{\text{pg}}} \right)^6 \right] \quad (9)$$

where  $r_{\text{pg}}$  and  $\sigma_{\text{pg}} = (\sigma + \sigma_g)/2$  are the center-to-center distance and equilibrium distance between sugar units, respectively. The dimensionless parameter  $H_{\text{pg}} = (B_i \times H)^{1/2}$ ; here  $H$  is the dimensionless parameter of glycan as shown in eq 7, and  $B_i$  is determined by the nature of amino acid; that is,  $B_i = 0$  if amino acid  $i$  is  $N_p$ ,  $B_i = -1$  if amino acid  $i$  is  $P_p$ , and  $B_i = 1$  if amino acid  $i$  is  $N_p$ .

Hydrogen binding, which plays an important role during glycoprotein folding and stability, is implicitly considered in the bonding potential and LJ-potential to maintain the structure of protein and attractive interaction between glycans and proteins.

**Simulation Methods.** Langevin dynamics and the velocity Verlet algorithm, using Gromacs 4.0 as the platform, were applied to examine the conformational transitions of the  $\beta$ -barrel protein and its glycosylated variants. The friction coefficient  $\gamma$  was set as 0.01. The protein configuration was updated in time steps of 0.0002 ps.

**Analytical Methods.** The root-mean-square deviation (rmsd) reflects the similarity of the specific conformation of a  $\beta$ -barrel protein conjugated with glycans to the native conformation obtained by the simulated annealing method and is obtained from eq 10:

$$\text{rmsd}(t, t_0) = \left[ \frac{1}{M} \sum_{i=1}^N m_i \|r_i(t) - r_i(t_0)\|^2 \right]^{1/2} \quad (10)$$

where  $m_i$  is the mass of amino acid residue  $i$  in the  $\beta$ -barrel protein,  $r_i(t)$  is the internal coordinate of amino acid residue  $i$  at time  $t$ , and  $r_i(t_0)$  is the internal coordinate of amino acid residue  $i$  in the initial state; that is, the native conformation.  $M = \sum_{i=1}^N m_i$  is the mass of the  $\beta$ -barrel protein. For the  $\beta$ -barrel protein, rmsd varies in the orders of nanometer. The lower rmsd indicates that the conformation is more similar to the native one. Note that only amino acid residues that determine the biological function of the protein in free or conjugated form are considered in the rmsd.

$T_f$  the folding temperature of the  $\beta$ -barrel protein and its glycosylated variants, is determined by the free-energy profile; at  $T_f$  the free energy of the native state is identical to that of the unfolded state. A higher  $T_f$  indicates a higher thermal stability.

The trajectories of the  $\beta$ -barrel protein and its glycosylated variants were obtained using a weighted histogram analysis method.<sup>46</sup> Only the energy term for the  $\beta$ -barrel protein was considered, to set an identical benchmark for the free and conjugated protein.

Folding yield (the fraction of native conformations) and average folding time (the time of first reaching the native conformation) were averaged from at least 1000 parallel simulations with different initial configurations.

## RESULTS AND DISCUSSION

**How Glycan Chains Affect the Conformational Stability of the Conjugated  $\beta$ -Barrel Protein.** We first examined the conformational stability of the  $\beta$ -barrel protein as a function of both the length and sites of glycans. The  $T_f$  of the  $\beta$ -barrel protein was determined to be 330 K. We then attached glycans with 14

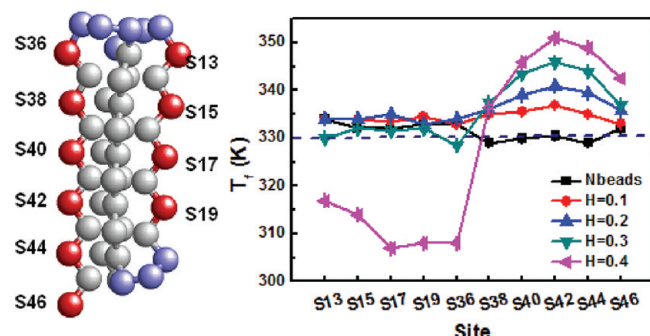


Figure 2. Folding temperature of different glycosylated variants of the  $\beta$ -barrel protein.

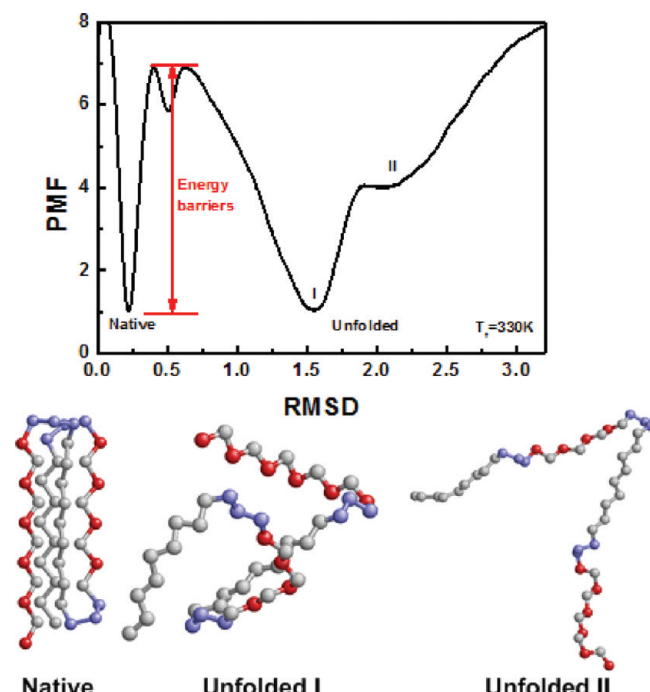


Figure 3. Free-energy profile and typical conformations of nonglycosylated  $\beta$ -barrel protein.

sugar units to 10 glycosylation sites on the protein surface. Figure 2 gives the  $T_f$  of the glycosylated  $\beta$ -barrel protein at different sites of glycosylation and hydrophobicities of glycan.

As shown in Figure 2a, the 10 glycosylation sites on the  $\beta$ -barrel protein can be classified into two categories. When glycosylation occurred at position 13, 15, 17, 19, or 36, N-type and weakly hydrophobic ( $H < 0.2$ ) glycans slightly elevated  $T_f$ , whereas strongly hydrophobic glycans ( $H > 0.2$ ) decreased  $T_f$ . The other type of glycosylation site comprises residues 38, 40, 42, 44, and 46. When glycosylation occurs at these sites, N-type glycans have no effect on  $T_f$ . An increase in the hydrophobicity of the glycans significantly elevated  $T_f$ , especially when glycosylation occurred on residue 42. A more detailed examination of the  $\beta$ -barrel protein indicated that residues 13, 15, 17, 19, and 36 have a common feature; that is, the mobility of these residues is constrained by their neighboring residues. By contrast, residues 38, 40, 42, 44, and 46 are on the ends of the polypeptide chains and are thus flexible. Above simulation results indicate that, when glycosylation occurs at the restricted peptide residues of protein

(residues 13, 15, 17, and 19), the glycan should be modeled with  $H = 0$  or very weak hydrophobicity ( $H < 0.2$ ). Once glycosylation occurs on the flexible part of protein (residue 40, 42, 44, and 46), the glycan should be modeled with  $H > 0$ . That is, both glycosylation sites and hydrophobicity of glycan commonly determine the structural transition of glycoproteins.

In published studies, glycoprotein stabilization results from a largely entropic rather than enthalpic effect.<sup>47</sup> That is, the glycan reduces the disorder of the unfolded protein, thereby destabilizing the unfolded state of the glycosylated protein compared with its native (i.e., nonglycosylated) counterpart.<sup>48</sup> DeKoster et al. observed a reduction of the melting temperature of the ovomucoid

first domain by 4.8 °C as a result of deglycosylation.<sup>49</sup> The magnitude of the enthalpy was essentially the same for both glycosylated and nonglycosylated ovomucoid; thus the stabilization effect of glycosylation was attributed to entropic factors. Similar conclusions have also been drawn for invertase, fetuin, and glucoamylase.<sup>50</sup> Using NMR with extensive nuclear Overhauser enhancement, Erbel et al.<sup>51</sup> have shown that the interaction between hydrophobic protein residues, such as Leu12, Ile25, Val68, and Val76, and the glycan backbone greatly affects the stability of glycosylated human chorionic gonadotropin hormone. The enhancement of stability of above proteins can be attributed to the glycosylation occurred at the restricted peptide

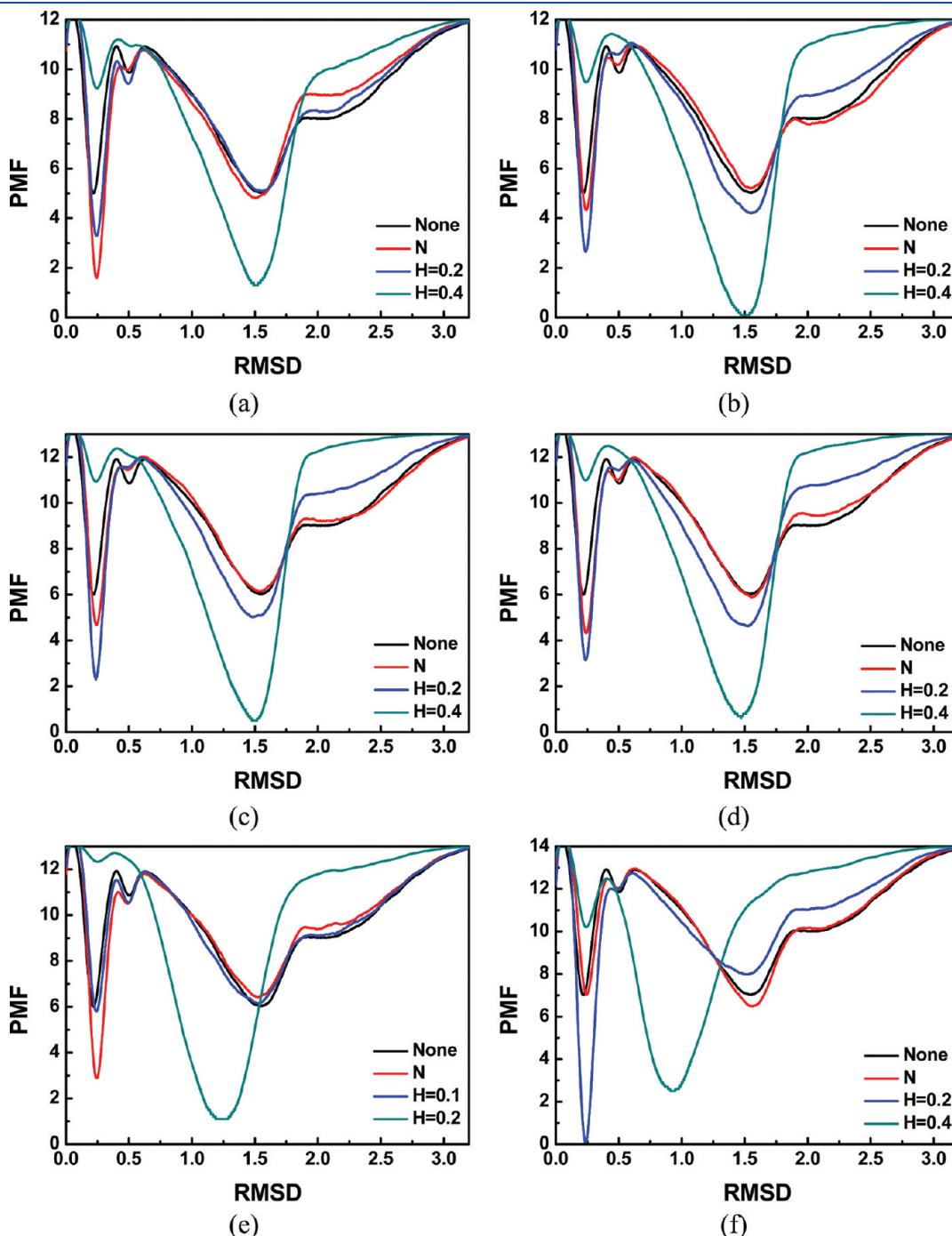
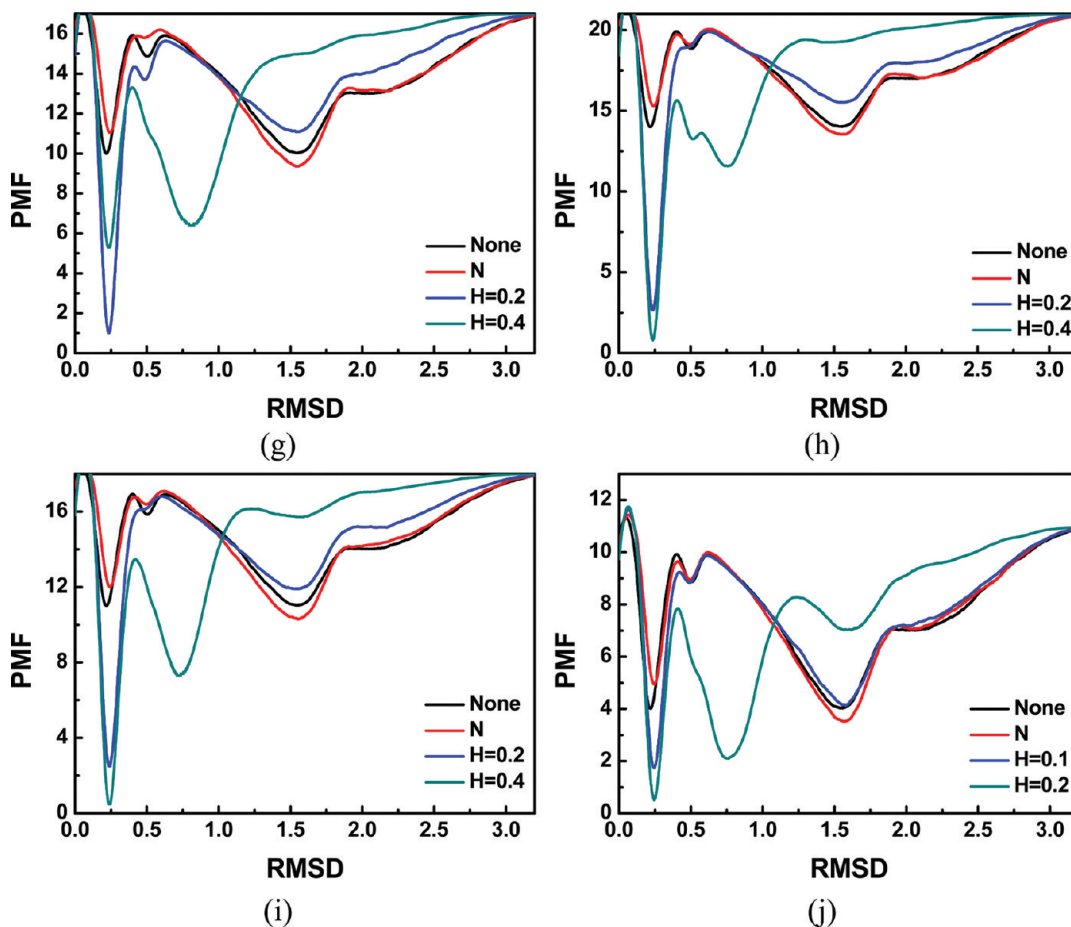


Figure 4. Continued



**Figure 4.** Free-energy profile plotted rmsd for  $\beta$ -barrel protein and its glycosylated variants. (a) S13; (b) S15; (c) S17; (d) S19; (e) S36; (f) S38; (g) S40; (h) S42; (i) S44; (j) S46.

residues. The introduction of glycan with repulse force between protein and glycan cannot alter the enthalpy of protein but narrow the conformation space of unfolded protein, that is, the entropic effect. This is one of specific cases in our simple glycoprotein model. However, there are also cases where glycosylation has no effect on thermal stability. For example, Wang et al. reported that glycosylation had no effect on the melting temperature of avidin and ovotransferrin.<sup>50</sup> More interestingly, Chen et al. studied the folding energy landscape of the bacterial immunity protein Im7 using site-specific N-linked glycosylation.<sup>52</sup> It was shown that  $\Delta\Delta G^0$  values for glycan incorporation ranged from +5.2 to  $-3.8 \text{ kJ}\cdot\text{mol}^{-1}$ . This indicated that stabilization or destabilization after glycosylation was highly dependent on the position and properties of the glycan chain, which is consistent with our simulation results shown in Figure 2. Similar experimental results have been obtained for other proteins, such as bovine Pofut1<sup>53</sup> and ovalbumin.<sup>54</sup> The above simulation results, though obtained from the coarse-grained model, are helpful for the design of glycosylated proteins for an enhanced stability.

**How Glycan Chains Affect the Free Energy Landscape of the Conjugated  $\beta$ -Barrel Protein.** Figure 3 shows the free-energy profile of nonglycosylated  $\beta$ -barrel protein at  $T_f$ . The profile is divided by energy barriers into two major regions: the native versus the unfolded region. The typical native conformation is shown in the bottom left of Figure 3. The unfolded region can be further divided into two parts: the unfolded I and unfolded

II regions, whose typical conformations are shown in the bottom middle and bottom right of Figure 3, respectively. The unfolded I region encompasses proteins with a partially folded core comprising residues 13–32, whereas the proteins in unfolded II have a fully extended conformation. Such differences in the unfolded state underpin the diverse folding and aggregation behavior, as revealed by molecular simulation observed in our previous studies.<sup>45</sup>

The free-energy landscapes describing the folding of native  $\beta$ -barrel protein and  $\beta$ -barrel protein glycosylated with the glycans of differing hydrophobicity were simulated and described in terms of rmsd versus PMF. The results are given in Figure 4, in which a fixed  $T_f$  is ascribed to the native  $\beta$ -barrel protein. For clarity, Figure 4 shows only the native  $\beta$ -barrel protein, as a reference, and  $\beta$ -barrel protein glycosylated with N-type glycans (i.e.,  $H = 0.0$ ),  $H = 0.2$  and  $H = 0.4$ .

Figure 4a–d shows that the presence of N-type and weakly hydrophobic glycans mainly affected the free-energy landscape of unfolded II, when glycosylation occurred at residues 13, 15, 17 and 19, which are restricted peptide residues. For N-type glycans, the interaction between glycan and polypeptide is repulsive, which elevates the free energy of unfolded II while decreasing the free energy of the native state. This favors the conformational transition from the unfolded state to the native state and thus increases the stability of the native protein. As shown in Figure 3, glycosylation at residues 13, 15, 17, and 19 constrained the unfolded state as a result of the repulsive force between the glycan

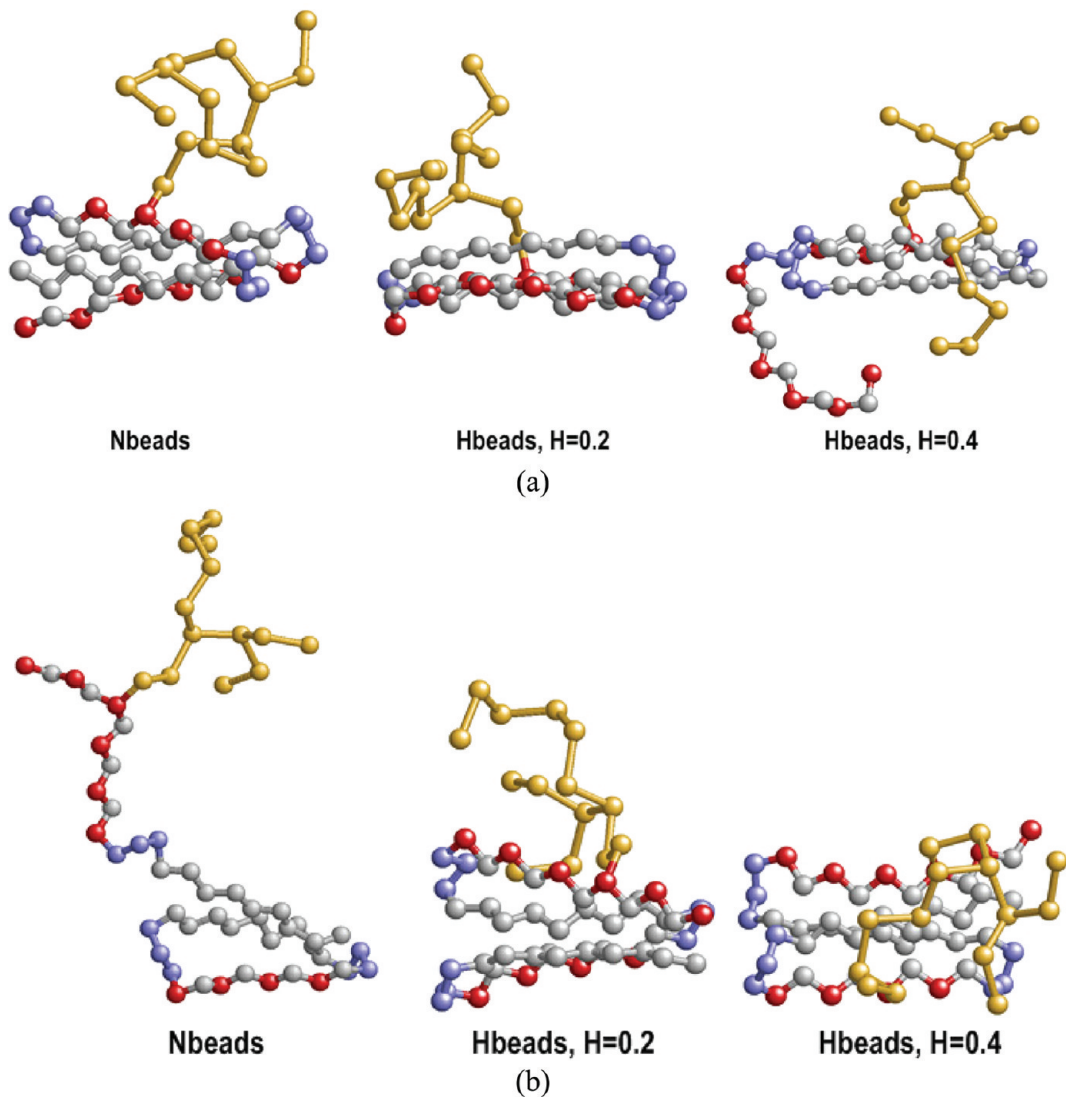


**Figure 5.** Typical conformations of different glycosylated  $\beta$ -barrel proteins. (a) Glycosylation at residue 17. (b) Glycosylation at residue 42.

and the polypeptide chains (or the glycan occupying the conformational space). These findings lead to the conclusion that the stabilization of glycosylated protein with restricted polypeptide residues may be entropic, in which the presence of the glycan chains constrains the conformational space available for the unfolded state. For weakly hydrophobic glycans ( $H < 0.2$ ), the glycan decreases not only the free energy of the native state, but also that of unfolded I states by increasing the free energy of the unfolded II state. In this case, both enthalpic and entropic effects act to improve protein stability. Whereas the entropic driving force increases the free energy of extended unfolded states, the enthalpic force is a “double-edged sword”. The hydrophobic interaction between polypeptide and glycan on the one hand reinforces unfolded I states by decreasing their free energy but on the other hand restricts the conformational transition of both glycan chain and protein. For strongly hydrophobic glycans ( $H = 0.4$ ), the enthalpic driving force is dominant; this “freezes” the protein in the unfolded I state via a strong interaction between glycan and polypeptide, leading to an increase in the free energy of both native and unfolded II states.

Figure 4a–d shows that glycosylation at residues 13, 15, 17, or 19 does not reduce the energy barrier between unfolded and

native states; on the contrary, this energy barrier may increase in the case of glycans with strong hydrophobicity and consequently hinder the folding or stability of the glycosylated protein, as discussed below.

Figure 4f–g shows that the presence of N-type glycans (repulsive force) at residue 38, 40, 42, 44, or 46 does not alter the free-energy landscape of the  $\beta$ -barrel protein. Once glycans of suitable hydrophobicity (e.g.,  $H = 0.2$  or  $H = 0.3$ ) are introduced, the free energy of native state is reduced while the free energy of unfolded state, including unfolded I and unfolded II, is increased. This favors folding toward the native conformation. Although the introduction of glycans with strong hydrophobicity (e.g.,  $H = 0.4$ ) also increases the free energy of the unfolded state, partially folded states ( $rmsd = 0.5–1.0$ ) also appear, which indicates that the intermediate state of the protein is stabilized through a strong hydrophobic interaction with glycans. This suggests that the stabilization of both the native glycosylated protein and the partially folded states is enthalpic, and thus hydrophobic interaction with the glycans stabilizes the model protein.

The influence of the glycosylation site on the stabilization effects of the glycans is noteworthy. In the model protein used in

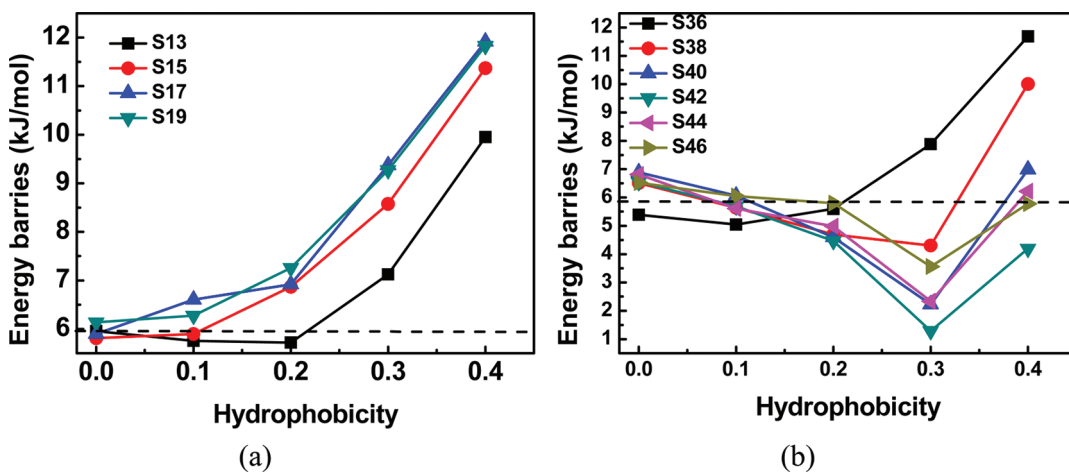


Figure 6. Free-energy barriers between the unfolded and folded states of different glycosylated  $\beta$ -barrel proteins (the broken line is the free-energy barrier between unfolded and native nonglycosylated  $\beta$ -barrel protein). (a) Glycosylation at residue 13, 15, 17, or 19; (b) Glycosylation at residue 36, 38, 40, 41, 44, or 46.

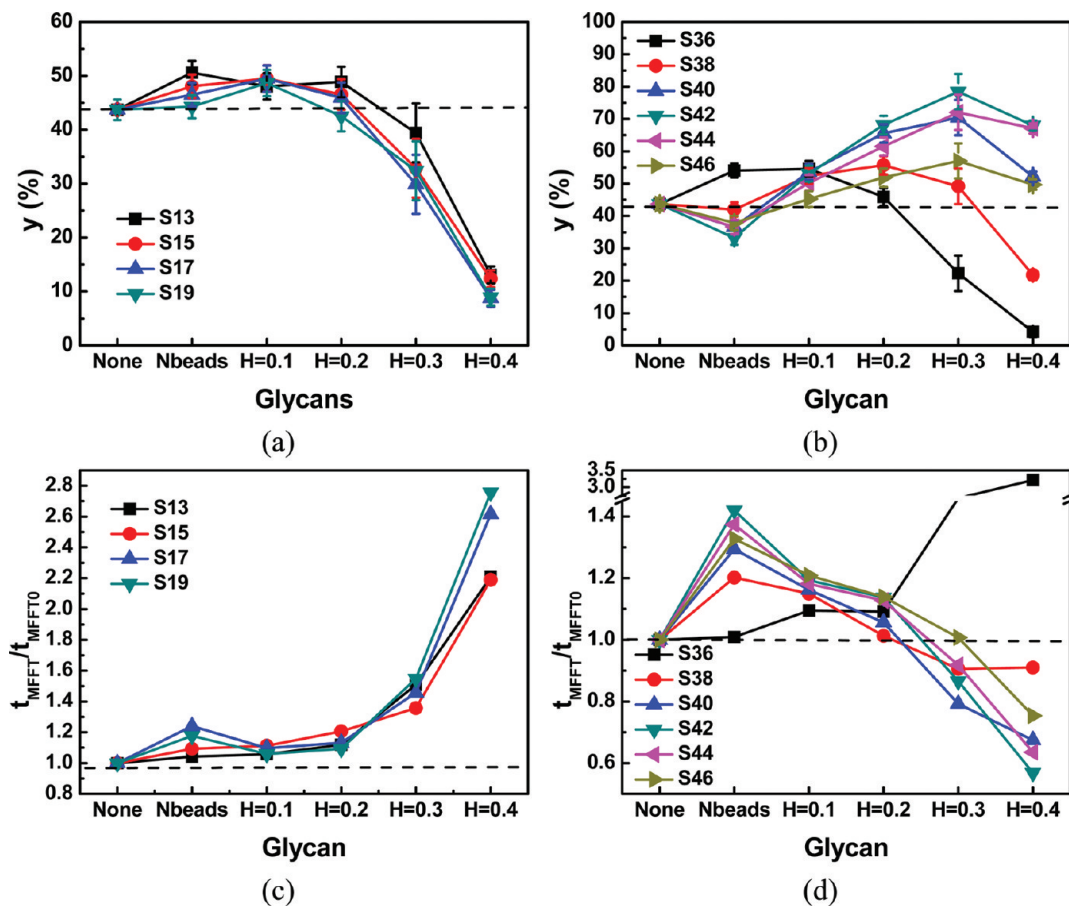
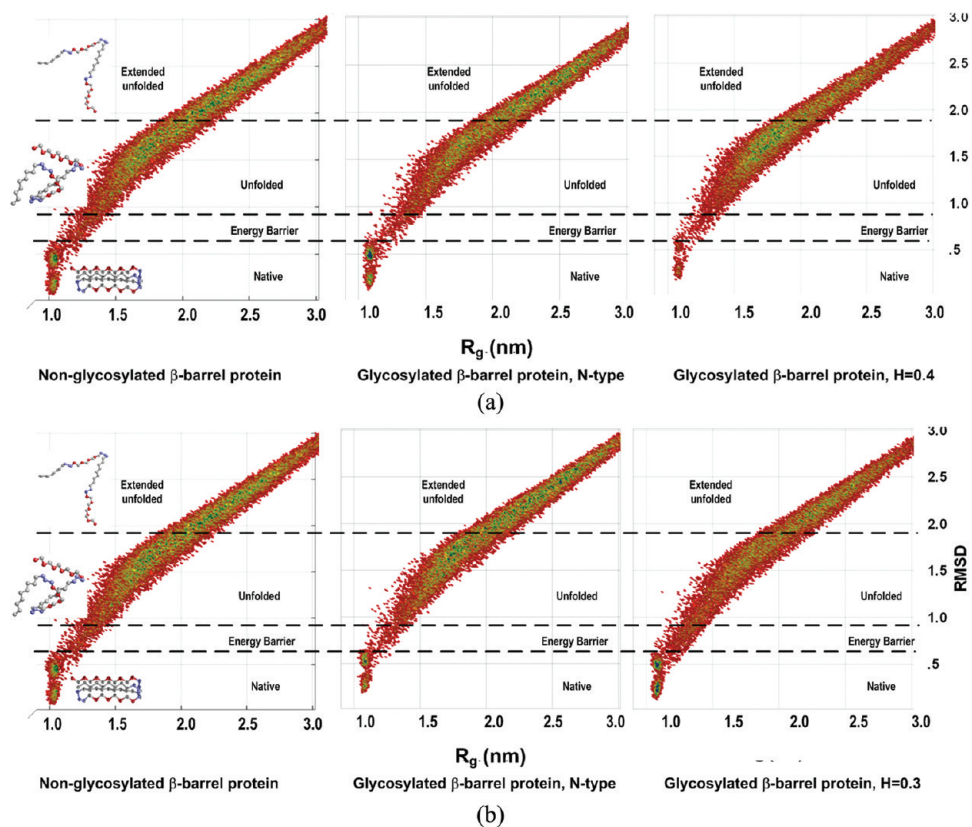


Figure 7. Folding yield and relative folding time of glycosylated  $\beta$ -barrel protein as a function of hydrophobicity of glycan chains (the broken line indicates the nonglycosylated  $\beta$ -barrel protein). (a) Folding yield of  $\beta$ -barrel proteins glycosylated at residue 13, 15, 17, or 19. (b) Folding yield of  $\beta$ -barrel proteins glycosylated at residue 36, 38, 40, 42, 44, or 46. (c) Relative folding time of  $\beta$ -barrel proteins glycosylated at residue 13, 15, 17, or 19. (d) Relative folding time of  $\beta$ -barrel proteins glycosylated at residue 36, 38, 40, 42, 44, or 46.

In the present study, glycosylation occurred at residue 42, irrespective of the hydrophobicity of the glycan, significantly increases the stability of the  $\beta$ -barrel protein, as shown in Figures 2 and 4h. This may be attributed to the way the glycan is entangled around

the protein, as shown in Figure 5b. Figure 4f–g also shows that glycosylation, at the above-mentioned residues, reduces the magnitude of the energy barrier between the unfolded and the native states, facilitating protein folding into the native conformation.



**Figure 8.** Folding maps of  $\beta$ -barrel glycoproteins with different glycosylated sites. (a) Glycosylated at residue 13. (b) Glycosylated at residue 42.

The function of glycans in assisting protein folding has been reported experimentally elsewhere.<sup>55–58</sup>

It is also interesting that, as shown in Figure 4e, glycosylation at residue 36 gives the  $\beta$ -barrel protein a  $T_f$  similar to that with glycosylation at residue 13, 15, 17, or 19 (Figure 2) but a free-energy landscape similar to that with glycosylation at residue 38, 40, 42, 44, or 46. This may be attributed to the position of residue 36, which is located on the turn of the  $\beta$ -barrel protein (Figure 2), and further illustrates the impact of glycosylation site on the properties of the core protein.

**Glycosylated  $\beta$ -Barrel Proteins: A Molecular View.** Figure 5 shows the typical conformations of different glycosylated  $\beta$ -barrel proteins at 300 K.

Figure 5a shows the conformations of glycoprotein glycosylated at residue 17. When the glycan is hydrophilic or weakly hydrophobic, its introduction not only increases the entropy of the protein–glycan conjugate by the addition of the freedom of the glycan but also slightly restricts protein fluctuation, thus increasing the stability of the glycoprotein. When glycans are strongly hydrophobic, however, the strong interaction between the glycan and the hydrophobic core of the protein deforms the native structure of the protein, thus decreasing protein stability.

Figure 5b shows the conformations of glycoprotein glycosylated at residue 42. When the glycan is hydrophilic, the repulsive force between protein and glycan results in the deformation of the side chain from the hydrophobic core of the protein, leading to destabilization of the protein. When the glycan has the appropriate hydrophobicity, the interaction between the protein and hydrophobic patches of the protein “fixes” the flexible chain around the protein by the formation of an “entangled structure”,

leading to a significant increase of protein stability, as shown in Figure 2.

**Folding of Glycosylated  $\beta$ -Barrel Protein.** Figure 6 shows the free-energy barriers between the unfolded and the folded states of different glycosylated  $\beta$ -barrel proteins.

As shown in Figure 6a, when glycosylation occurred at residue 13, 15, 17 or 19, the free-energy barrier increased with the hydrophobicity of the glycan. In the case of glycosylation at residue 13, the free-energy barrier decreased slightly when the glycan chain was neutral or weakly hydrophobic ( $H < 0.2$ ), implying a slightly acceleratory of folding rate. In general, glycosylation at residue 13, 15, 17, or 19 does not facilitate or hinder protein folding.

In Figure 6b, it is seen that, when glycosylation occurred at residue 36, the free-energy barrier decreased slightly with increased values of  $H$ , reaching a minimum at  $H = 0.1$ , and then increased sharply. This behavior resembles that of the  $\beta$ -barrel protein glycosylated at residue 13. According to Figure 2, residues 13 and 36 are both near the turn of the  $\beta$ -barrel protein.

Figure 6b shows that, when glycosylation occurred at residue 38, 40, 42, 44, or 46, the free-energy barrier first decreases with increasing values of  $H$ , reaching a minimum at  $H = 0.3$ , then increases; this indicates that glycans of appropriate hydrophobicity can accelerate  $\beta$ -barrel protein folding significantly. That is to say, with the appropriate hydrophobicity, and modifying the appropriate residues, glycan chains can function as “molecular chaperones”.

**Glycans Can Significantly Affect  $\beta$ -Barrel Protein Folding Yield and Folding Rate.** We then simulated the folding of different  $\beta$ -barrel proteins at 315 K. The folding yields and relative average folding times (denoted as  $t_{\text{MFPT}}/t_{\text{MMFT0}}$ ) are shown in Figure 7.

Figure 7a,b shows that, when glycosylation occurred at site 13, 15, 17, 19 or 36, hydrophilic glycans ( $N$  type) and weakly hydrophobic glycans ( $H < 0.2$ ) only slightly improved the folding yield. When glycosylation occurred at site 38, 40, 42, 44 or 46, however, relatively strongly hydrophobic glycans ( $H = 0.2–0.3$ ) significantly improved the folding yield. It is also shown in Figure 7a,b that, when glycosylation occurred at site 42 with  $H = 0.3$ , the folding yield reached a maximum, indicating that the folding yield of glycoprotein can be significantly influenced by both the site of glycosylation and the properties of the glycan.

Figure 7c,d shows the relative average folding time as a function of glycan hydrophobicity at different glycosylation sites. When glycosylation occurs at site 13, 15, 17, 19, or 36, the average folding time increased with increased glycan hydrophobicity. Considering this result together with Figure 7a,b, although hydrophilic and weakly hydrophobic glycans can slightly improve the folding yield, they can hinder the structural transition from the unfolded to the native state, leading to an increased folding time. When glycosylation occurs at site 38, 40, 42, 44, or 46, however, hydrophilic or weakly hydrophobic glycans increase the folding time and thus hinder protein folding, but relatively strongly hydrophobic glycans decrease the folding time and thus accelerate protein folding.

**Folding Maps of  $\beta$ -Barrel Protein and Its Glycosylated Variants.** Figure 8a,b shows folding maps of  $\beta$ -barrel glycoproteins glycosylated at sites 13 and 42, respectively.

As shown in Figure 8a, the folding maps can be divided into four regions: native, energy barrier, unfolded, and extended unfolded. The deeper the green color, the greater the number of conformations in the region; the white color indicates no conformations. When residue 13 was glycosylated with an N-type glycan, the number of conformations in the region of the energy barrier decreased, indicating an increase of the energy barrier and thus hindering protein folding. In addition, more conformations appeared in the native region, indicating a high folding yield. This is consistent with the results shown in Figures 6 and 7. Thus, N-type glycans improve the folding yield but decrease the folding rate when glycosylation occurs at residue 13. When a strongly hydrophobic glycan is grafted to residue 13, fewer conformations appear not only in the energy barrier region, but also in the native region, indicating that this type of glycoprotein gives a low folding yield and high energy barriers between native and unfolded states, leading to the slow folding rate. It is also shown that more conformations appear in the unfolded region, and fewer conformations appear in the extended region. This indicates that the number of collapsed unfolded conformations is increased because of the strong hydrophobic interaction between glycan and protein.

Figure 8b gives the folding maps of glycoprotein glycosylated at residue 42. When glycosylated with N-type glycan, conformations in both the energy barrier region and the native region decrease, indicating a lower folding yield and slower folding rate. This is consistent with the results shown in Figures 6 and 7. Following glycosylation with an appropriately hydrophobic glycan ( $H = 0.3$ ), more conformations appear in both the energy barrier and the native region, indicating an improved folding yield and acceleration of folding.

## CONCLUSION

In this article, we explored the thermodynamics and folding kinetics of glycoprotein with different types of glycans using a

coarse-grained model and molecular dynamics simulations, in which an  $H$  term was proposed as the index of the hydrophobicity of glycan. Both stabilization and destabilization effects of glycans on protein were displayed. The introduction of branched glycans of appropriate hydrophobicity not only increased conformational stability but also increased foldability compared with the native counterpart. A complex relationship was observed between thermal stabilization of protein by glycan chains and the hydrophobicity and glycosylation sites of chains attached. It was shown that both the hydrophobicity of the glycan and the glycosylation site affected significantly the folding and stability of this glycosylated protein. Compared with its native counterpart, introducing glycans of suitable hydrophobicity ( $0.1 < H < 0.4$ ) at flexible peptide residues of model protein not only facilitated folding of the model protein but also increased its conformational stability significantly. On the contrary, introducing glycans at the restricted peptide residues of model protein, only those hydrophilic ( $H = 0$ ) or very weak hydrophobic ( $H < 0.2$ ) glycans can slightly enhance protein stability but hinders protein folding due to increased free energy barrier. In addition to an entropy effect, that is, narrowing the conformational space of the unfolded state, the presence of glycans with suitable hydrophobicity at suitable glycosylation site strengthened the folded state via hydrophobic interaction, that is, the enthalpy effect. Folding trajectories suggested that the model protein had a two-step folding mechanism in terms of hydrophobic collapse and structural rearrangement. Glycan chains of appropriate hydrophobicity located in specific sites could both accelerate protein collapse and facilitate protein rearrangement, while some glycan chains could only accelerate protein collapse and hinder protein rearrangement. In summary, the stability and folding behavior of the glycosylated protein, which can be viewed as protein-glycan conjugate, is determined by both the location and the hydrophobicity of glycosylated chain. As for the model protein of the present study, hydrophilic and weakly hydrophobic glycans located at the restricted peptide residues (such as residues 13, 15, 17, and 19 in our simulations) enhance stability of protein via compressing the conformational space of unfolded protein, which could be attributed to the entropic effect via the excluded volume effect. The folding yield of glycosylated protein, however, could be increased at a compromise folding rate. On the other hand, glycans with a suitable hydrophobicity located at the flexible region of the protein (such as residues 38, 40, 42, 44, and 46 in our simulations) could enhance both the stability and folding rate and yield of the model protein. This could be attributed to the hydrophobic interaction between protein and glycan and described in terms of the enthalpy effect. It is noted here that while hydrogen bonding, an essential interaction between glycans and polypeptides, is implicitly considered in above-mentioned model, a full display of the effects of hydrogen bonding on the stability and folding properties of proteins requires an all-atom model. Nevertheless, the above simulation has provided molecular level insight into diversified effects of glycosylation, as experimentally reported elsewhere,<sup>47–54</sup> which is helpful for the design and synthesis of protein–glycan conjugates for various applications.

## AUTHOR INFORMATION

### Corresponding Author

\*Tel.: 86-10-62779876. Fax: 86-10-62770304. E-mail: liuzheng@mail.tsinghua.edu.cn

## ■ ACKNOWLEDGMENT

This work was supported by National Natural Science Foundation of China under Grant No. 20706032, by National Excellent Doctoral Dissertation of PR China under Grant No. 200956, and by the Ministry of Science and Technology through 973 Project under Grant No. 2009CB724702.

## ■ REFERENCES

- (1) Pearse, B. R.; Hebert, D. N. *Biochim. Biophys. Acta* **2010**, *1803*, 684–693.
- (2) Shental-Bechor, D.; Levy, Y. *Curr. Opin. Struct. Biol.* **2009**, *19*, 524–533.
- (3) Petrescu, A. J.; Wormald, M. R.; Dwek, R. A. *Curr. Opin. Struct. Biol.* **2006**, *16*, 600–607.
- (4) Mitra, N.; Sinha, S.; Ramya, T. N. C.; Surolia, A. *Trends Biochem. Sci.* **2006**, *31*, 156–163.
- (5) Wyss, D. F.; Wagner, G. *Curr. Opin. Biotechnol.* **1996**, *7*, 409–416.
- (6) Soussillane, P.; D'Alessio, C.; Paccalet, T.; Fitchette, A. C.; Parodi, A. J.; Williamson, R.; Plasson, C.; Faye, L.; Gomord, V. *Glycoconjugate J.* **2009**, *26*, 597–607.
- (7) D'Alessio, C.; Caramelo, J. J.; Parodi, A. J. *Semin. Cell Dev. Biol.* **2010**, *21*, 491–499.
- (8) Berger, S.; Menudier, A.; Julien, R.; Karamanos, Y. *Phytochemistry* **1995**, *39*, 481–487.
- (9) Barraud, J. P.; Bourgerie, S.; Julien, R.; Guespinmichel, J. F.; Karamanos, Y. *J. Bacteriol.* **1995**, *177*, 916–920.
- (10) Zhou, F. F.; Xu, W.; Hong, M.; Pan, Z.; Sinko, P. J.; Ma, J. J.; You, G. F. *Mol. Pharmacol.* **2005**, *67*, 868–876.
- (11) Adak, A. K.; Leonov, A. P.; Ding, N.; Thundimadathil, J.; Kularatne, S.; Low, P. S.; Wei, A. *Bioconjugate Chem.* **2010**, *21*, 2065–2075.
- (12) Torosantucci, A.; Bromuro, C.; Chiani, P.; De Bernardis, F.; Berti, F.; Galli, C.; Norelli, F.; Bellucci, C.; Polonelli, L.; Costantino, P.; Rappuoli, R.; Cassone, A. *J. Exp. Med.* **2005**, *202*, 597–606.
- (13) Hackenberger, C. P. R.; Friel, C. T.; Radford, S. E.; Imperiali, B. *J. Am. Chem. Soc.* **2005**, *127*, 12882–12889.
- (14) Visciano, M.; Tagliamonte, M.; Tornesello, M.; Lopalco, L.; Buonaguro, F.; Buonaguro, L. *AIDS Res. Hum. Retroviruses* **2010**, *26*, A134–A135.
- (15) Jang, B. C.; Sung, S. H.; Park, J. G.; Park, J. W.; Bae, J. H.; Shin, D. H.; Park, G. Y.; Han, S. B.; Suh, S. I. *J. Biol. Chem.* **2007**, *282*, 27622–27632.
- (16) Moll, M.; Kaufmann, A.; Maisner, A. *J. Virol.* **2004**, *78*, 7274–7278.
- (17) Helenius, A.; Aeby, M. *Annu. Rev. Biochem.* **2004**, *73*, 1019–1049.
- (18) Labasque, M.; Faivre-Sarrailh, C. *FEBS Lett.* **2010**, *584*, 1787–1792.
- (19) Chatterjee, S.; Mayor, S. *Cell. Mol. Life Sci.* **2001**, *58*, 1969–1987.
- (20) Nasirud, D.; Ahmad, I.; Hoessli, D. C.; Walker-Nasir, E.; Choudhary, M. I. *Curr. Org. Chem.* **2007**, *11*, 609–618.
- (21) Jeanneau, C.; Chazalet, V.; Auge, C.; Soumpasis, D. M.; Harduin-Lepers, A.; Delannoy, P.; Imbert, A.; Breton, C. *J. Biol. Chem.* **2004**, *279*, 13461–13468.
- (22) Martina, J. A.; Daniotti, J. L.; Macchioni, H. J. F. *J. Neurochem.* **1997**, *69*, S11–S11.
- (23) Helle, F.; Dubuisson, J. *Virologie* **2009**, *13*, 271–282.
- (24) Katsuma, S.; Nakanishi, T.; Daimon, T.; Shimada, T. *J. Gen. Virol.* **2009**, *90*, 170–176.
- (25) Wujek, P.; Kida, E.; Walus, M.; Wisniewski, K. E.; Golabek, A. A. *J. Biol. Chem.* **2004**, *279*, 12827–12839.
- (26) Ryu, K. S.; Lee, J. O.; Kwon, T. H.; Choi, H. H.; Park, H. S.; Hwang, S. K.; Lee, Z. W.; Lee, K. B.; Han, Y. H.; Choi, Y. S.; Jeon, Y. H.; Cheong, C.; Kim, S. *Biochem. J.* **2009**, *421*, 87–96.
- (27) Tie, J. K.; Zheng, M. Y.; Pope, R. M.; Straight, D. L.; Stafford, D. W. *Biochemistry* **2006**, *45*, 14755–14763.
- (28) Cheng, S. M.; Edwards, S. A.; Jiang, Y. D.; Grater, F. *ChemPhysChem* **2010**, *11*, 2367–2374.
- (29) Knudsen, S. K.; Stensballe, A.; Franzmann, M.; Westergaard, U. B.; Otzen, D. E. *Biochem. J.* **2008**, *412*, 563–577.
- (30) Price, J. L.; Shental-Bechor, D.; Dhar, A.; Turner, M. J.; Powers, E. T.; Gruebele, M.; Levy, Y.; Kelly, J. W. *J. Am. Chem. Soc.* **2010**, *132*, 15359–15367.
- (31) Hanson, S. R.; Culyba, E. K.; Hsu, T. L.; Wong, C. H.; Kelly, J. W.; Powers, E. T. *Proc. Natl. Acad. Sci. U.S.A.* **2009**, *106*, 3131–3136.
- (32) Meng, J.; Parroche, P.; Golenbock, D. T.; McKnight, C. J. *J. Biol. Chem.* **2008**, *283*, 3376–3384.
- (33) Gupta, G.; Sinha, S.; Mitra, N.; Surolia, A. *Glycoconjugate J.* **2009**, *26*, 691–695.
- (34) Xu, Y. Q.; Bartido, S.; Setaluri, V.; Qin, J.; Yang, G.; Houghton, A. N. *Exp. Cell Res.* **2001**, *267*, 115–125.
- (35) Choi, Y.; Lee, J.; Hwang, S.; Kim, J. K.; Jeong, K.; Jung, S. *Biopolymers* **2008**, *89*, 114–123.
- (36) Fernandez-Tejada, A.; Corzana, F.; Bustos, J. H.; Avenoza, A.; Peregrina, J. M. *J. Org. Chem.* **2009**, *74*, 9305–9313.
- (37) Fernandez-Tejada, A.; Corzana, F.; Bustos, J. H.; Avenoza, A.; Peregrina, J. M. *Org. Biomol. Chem.* **2009**, *7*, 2885–2893.
- (38) Shental-Bechor, D.; Levy, Y. *Proc. Natl. Acad. Sci. U.S.A.* **2008**, *105*, 8256–8261.
- (39) Lu, D.; Liu, Z. *J. Phys. Chem. B* **2008**, *112*, 15127–15133.
- (40) Klimov, D. K.; Newfield, D.; Thirumalai, D. *Proc. Natl. Acad. Sci. U.S.A.* **2002**, *99*, 8019–8024.
- (41) Lu, D. N.; Liu, Z.; Wu, J. *Z. Biophys. J.* **2006**, *90*, 3224–3238.
- (42) Zhang, L.; Lu, D. N.; Liu, Z. *J. Chromatogr., A* **2009**, *1216*, 2483–2490.
- (43) Lu, D.; Wu, J.; Liu, Z. *J. Phys. Chem. B* **2007**, *111*, 12303–12309.
- (44) Lu, D. N.; Liu, Z.; Wu, J. *Z. J. Chem. Phys.* **2007**, *126*, 064906.
- (45) Lu, D. N.; Liu, Z. *J. Phys. Chem. B* **2008**, *112*, 2686–2693.
- (46) Tipping, E. *Comput. Geosci.* **1994**, *20*, 973–1023.
- (47) Xu, G. Q.; Narayan, M.; Scheraga, H. A. *Biochemistry* **2005**, *44*, 9817–9823.
- (48) Mendez, D. L.; Jensen, R. A.; McElroy, L. A.; Pena, J. M.; Esquerre, R. M. *Arch. Biochem. Biophys.* **2005**, *444*, 92–99.
- (49) DeKoster, G. T.; Robertson, A. D. *Biochemistry* **1997**, *36*, 2323–2331.
- (50) Wang, C. Q.; Eufemi, M.; Turano, C.; Giartosio, A. *Biochemistry* **1996**, *35*, 7299–7307.
- (51) Erbel, P. J. A.; Karimi-Nejad, Y.; De Beer, T.; Boelens, R.; Kamerling, J. P.; Vliegenthart, J. F. G. *Eur. J. Biochem.* **1999**, *260*, 490–498.
- (52) Chen, M. M.; Bartlett, A. I.; Nerenberg, P. S.; Friel, C. T.; Hackenberger, C. P. R.; Stultz, C. M.; Radford, S. E.; Imperiali, B. *Proc. Natl. Acad. Sci. U.S.A.* **2010**, *107*, 22528–22533.
- (53) Loriol, C.; Audfray, A.; Dupuy, F.; Germot, A.; Maftah, A. *FEBS J.* **2007**, *274*, 1202–1211.
- (54) Ito, K.; Ishimaru, T.; Kimura, F.; Matsudomi, N. *Biochem. Biophys. Res. Commun.* **2007**, *361*, 725–731.
- (55) McCormick, L. M.; Urade, R.; Arakaki, Y.; Schwartz, A. L.; Bu, G. J. *Biochemistry* **2005**, *44*, 5794–5803.
- (56) Okajima, T.; Xu, A. G.; Lei, L.; Irvine, K. D. *Science* **2005**, *307*, 1599–1603.
- (57) Lee, J.; Di Jeso, B.; Arvan, P. *J. Clin. Invest.* **2008**, *118*, 2950–2958.
- (58) Mackeen, M. M.; Almond, A.; Deschamps, M.; Cumpstey, I.; Fairbanks, A. J.; Tsang, C.; Rudd, P. M.; Butters, T. D.; Dwek, R. A.; Wormald, M. R. *J. Mol. Biol.* **2009**, *387*, 335–347.